Field investigations for evaluating green infrastructure effects on air quality in open-road conditions

KV Abhijith, Prashant Kumar*

Global Centre for Clean Air Research (GARE), Department of Civil and Environmental Engineering, Faculty of Engineering and Physical Sciences, University of Surrey, Guildford GU2 7XH, United Kingdom

Graphical abstract

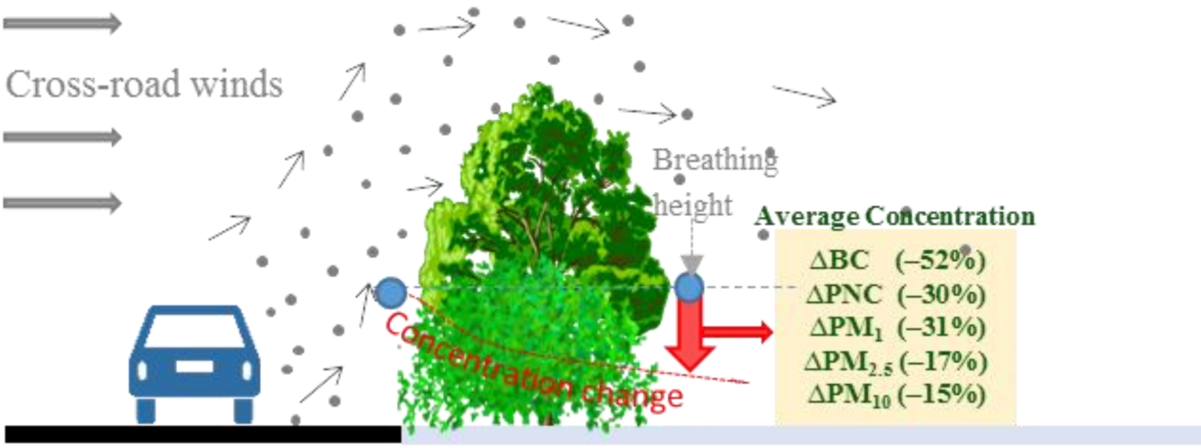

Abstract

Many people live, work and spend time during their commute in near-road environments (<50 m) where pollutant concentrations usually remain high. We investigated the influence of roadside green infrastructure (GI) on concentrations of particulate matter ≤10 µm (PM_{10}), ≤2.5 µm ($PM_{2.5}$), ≤1 µm (PM_1), black carbon (BC) and particle number concentrations (PNC) under three GI configurations – (i) hedges only, (ii) trees only, and (iii) a mix of trees and

*Corresponding author. Address as above. Email: p.kumar@surrey.ac.uk; Prashant.Kumar@cantab.net

hedges/shrubs – separately in close (<1m) and away (>2m) road conditions. These configurations gave us a total of six different real-world scenarios for evaluation. The changes in concentrations of PM_{10}, $PM_{2.5}$, PM_1, BC and PNC at all six sites were estimated by comparing simultaneous measurements behind and in front of GI (or adjacent clear area). A portable battery-operated experimental set-up was designed for measuring the pollutant concentrations for 30 full days over a field campaign period of three months. On each day, around 10 hours of continuous data were recorded simultaneously behind and in front of GI/ adjacent clear area, capturing both morning and evening traffic peaks. Our objectives were to: (i) assess the effectiveness of different types of GI in reducing various pollutants; (ii) evaluate the impact of wind directions and density of vegetation on reducing different pollutant concentrations behind GI; (iii) investigate the changes in fractional composition of sub-micron (PM_1), fine ($PM_{2.5}$) and coarse ($PM_{2.5-10}$) particles; and (iv) quantify the elemental composition of collected particles before and after the GI. In away-road conditions, all three configurations showed reductions behind the GI for all pollutants. The 'hedges only' configuration showed higher pollutant reductions than the other two configurations, with maximum reductions of up to 63% shown for BC. In close-road conditions, the results were mixed. The 'trees only' configuration reported increases in most of the pollutant concentrations, whereas the combination of trees and hedges resulted in reduced pollutant concentrations behind the GI. Among all pollutants, the highest relative changes in concentration were observed for BC (up to 63%) and lowest for $PM_{2.5}$ (14%). Categorising the data based on wind directions showed the highest reduction during along-road wind conditions (i.e., parallel to the road). This was expected due to the sweeping of emissions by the wind and the wake of road vehicles whilst the barrier effect of GI enhanced this cleansing, limiting lateral diffusion of the pollutants. However, cross-road winds that took vehicular emissions to pass through the GI allowed us to assess their influence, showing up to 52, 15, 17, 31 and 30% reduction for BC, PM_{10}, $PM_{2.5}$,

PM_1 and PNC, respectively. The largest reductions were consistently noted for the mixed 'trees and hedges' configuration in close-road conditions and the 'hedge only' configuration in away-road conditions. The assessment of various fractions of PM showed that 'hedges only' and a combination of trees and hedges lowered fine particles behind GI. The SEM-EDS analysis indicated the dominance of natural particles (50%) and a reduction in vehicle-related particles (i.e., iron and its oxides, Ba, Cr, Mn) behind GI when compared with the in-front/adjacent clear area. The evidence contributed by this work enhances our understanding of air quality modifications under the influence of different GI configurations, for multiple pollutants. In turn, this will support the formulation of appropriate guidelines for GI design, to reduce the air pollution exposure of those living, working or travelling near busy roads.

Keywords: Green infrastructure; Near-road; particulate matter deposition; Hedges and trees; Air quality

1. Introduction

More than half of the global population (~54%) lives in urban areas (United Nations, 2014), while this fraction increases to almost two thirds (72%) in the European Union (European Environment Agency, 2015). Air pollution levels in many European cities are above permissible limits (European Environment Agency, 2013; Guerreiro et al., 2016), making it one of the primary environmental health risks (European Environment Agency, 2015). Road vehicles are the dominant source of harmful ambient air pollutants, such as particulate matter (PM), nitrogen oxides (NO_x), carbon monoxide (CO) and volatile organic compounds (VOCs). Traffic-related air pollutants are emitted close to ground-level, causing elevated pollutant concentrations near busy roadsqq when compared with urban background concentrations (Goel and Kumar, 2016; Karner et al., 2010; Pasquier and André, 2017). These traffic-generated emissions contribute to increased air pollution exposure in 'on-road', 'near-road' and 'far-road' microenvironments (Batterman, 2013; Batterman et al., 2014). In on-road microenvironments, drivers, commuters, pedestrians, and cyclists are exposed to air pollution (Kumar et al., 2018a, 2018b). The near-road microenvironment extends over a few hundred meters from highways, including where people live, walk or cycle. The far-field environment is beyond several hundred meters from traffic.

A significant fraction of the population lives in the near-road environment. For example, 45 million people live or work within 100m from heavily used roadways in the US (EPA, 2016). Likewise, about 40% of the population in cities such as Toronto lives within 500m of an expressway or within 100m of a major road (HEI, 2010). The majority of people living in near-road environments are low-income residents or minorities (Carrier et al., 2014a; Tian et al., 2013). In addition, exposure to traffic-related air pollutants of vulnerable schoolchildren escalates concerns over air quality in the near-road region (Carrier et al., 2014b; Kim et al., 2004; Kumar et al., 2017; Sharma and Kumar, 2018). Numerous studies have demonstrated the association of adverse health impacts with people living in near-road conditions proximate to highways. The range of health implications includes exacerbation of asthma (Clark et al., 2010; Evans et al., 2014; Volk et al., 2011), impaired lung function (Laumbach and Kipen, 2012), cardiovascular morbidity and mortality (Brook et al., 2010; Cahill et al., 2011; Wilker et al., 2013), adverse birth outcomes (Michelle Wilhelm, Jo Kay Ghosh, Jason Su, Myles Cockburn, Michael Jerrett, 2012), and cognitive declines (HEI, 2010; Volk et al., 2011).

Numerous exposure assessment investigations have analysed pollutant concentration distribution in the near-road environment (Karner et al., 2010; Pasquier and André, 2017). Near-road pollutant concentration levels are affected by distance to the road, road configuration, meteorology, and adjacent infrastructure geometries such as noise barriers and GI. Usually, concentrations of pollutants including particulate matter ≤10 μm (PM_{10}) and particle number concentrations (PNC) decay rapidly with distance from the road (Karner et al., 2010; Pasquier and André, 2017). Depending on the type of pollutants, concentration reaches close to background levels by 80m to 600m from the road (Karner et al., 2010; Pasquier and André, 2017). Apart from a distance to the road, specific roadway characteristics such as elevated, at-grade, and depressed roads can also influence the pollutant concentration distribution near highways (Baldauf et al., 2013; Patton et al., 2014; Steffens et al., 2014). Moreover, meteorological conditions affect near-road pollutant concentrations (Pasquier and André, 2017). When wind direction is perpendicular to the road (i.e. wind flows from the road to the nearby areas), pollutants travel longer distances downwind than when winds are parallel or inclined to the road. Lower pollutant concentrations are observed during high wind speeds, and an opposite trend is observed for low wind speeds (Karner et al., 2010; Pasquier and André, 2017). In addition, stable atmospheric conditions in winter seasons induce higher pollutant concentrations as opposed to relatively unstable summer periods that are associated with a decrease in pollutant concentrations.

Regardless of pollutant type, geometrical and meteorological factors, pollutant concentration close to the traffic (<50m, near-road) remains up to half of the on-road levels. Reducing air pollution exposure in this near-road environment could be achieved by implementing passive control measures such as GI and low boundary walls (Abhijith et al., 2017; Baldauf, 2017; Gallagher et al., 2015). The greening of cities is favoured for exploiting their diverse health benefits and ecosystem services, yet clear guidelines are needed for their implementation at roadside environments. This study focuses on GI performance in lowering pollution concentrations in near-road environments (<50m, near-road). Table 1 shows a summary of previous field experimental studies on air pollution modifications of different GI types in near-road environments, based on the pollutant concentration decay trend with distance from traffic (Karner et al., 2010; Pasquier and André, 2017); an extended version is available as

Supplementary Information, SI, Table S1. Usually, the highest GI-induced improvement is observed for pollutants such as ultrafine particles (UFP), carbon monoxide (CO) and PM_{10}.

The literature reports varying level of differences in pollutant concentration depending on the GI type (Abhijith et al., 2017; Chen et al., 2015; Hagler et al., 2012). For example, some studies showed decreased concentrations due to hedges (Tiwary et al. 2008; Al-Dabbous and Kumar, 2014) whereas others showed that trees can result in both air quality deterioration (Tong et al., 2015; Morakinyo et al., 2016; Yli-Pelkonen et al., 2017) and improvement (Yin et al., 2011; Lin et al., 2016). Before drawing generalisations on the air quality benefits of GI, it is important to consider the type of pollutants evaluated and reflected in any associated guidelines.

The objectives of this work are to assess the air quality improvement potential of different types of GI in the near-road environment. We quantify and compare the pollutant reduction potential of three different GI categories (trees, hedges, and trees with hedges/shrubs) under close-road (<1m) and away-road (>2m) conditions. In this work, we have used the terms GI and vegetation interchangeably and the combination of hedges and trees are expressed as GI, depending on the context. In addition, we considered at least one pollutant from each decay trend category (Karner et al., 2010): PNC and BC (rapid decay in pollutant concentration normalised to edge of road concentration with distance from roadside), $PM_{2.5}$ (usually a gradual decay), and PM_{10} (no clear trend in decay). This enables us to reveal the probable difference in concentration reduction of each pollutant category for different GI types. We also inspected the influences of wind direction as well as GI characteristics such as leaf area density on pollutant reduction and quantified the elemental composition of PM to determine the changes in traffic-generated elements such as Fe, Ba, Cr and Mn by the GI.

2. Methodology

2.1 Site description

We selected six roadside locations in a typical UK town, Guildford, which is one of the most populated areas in the Guildford Borough under Surrey County (Surrey-i, 2015). Guildford Borough has a population of 137,183 (Surrey-i, 2015). The most popular mode of transportation is by car, which includes about 72% of total commutes and 42% of these journeys are between house to school (Al-Dabbous and Kumar, 2014). The sampling sites consisted of two sets of the following three GI configurations: (i) trees, (ii) hedges, and (iii) a combination of trees and hedges/shrubs. Site selection was based on the availability of stretches of road with different GI configurations, as well as space for placing instruments behind GI and at an adjacent clear area or in front of GI. Fig 1 shows a schematic representation of monitoring locations along with the dimensions of GI, distance from the edge of the road to monitoring point, and width of traffic lanes. Table 2 lists a detailed summary of monitoring location features including highways and GI characteristics while an additional description is provided in SI Section SI. Each site had one sampling point behind the GI. In half of the sites, the second measurement point was at a clear area next to the GI, equidistant from the road as that of the sampling point behind the barrier (Figs 1a, c, e), and the remaining sites each had a second measurement location in front of the GI (Figs 1b, d, f). The sites with monitoring points at an adjacent clear area and behind GI (Figs 1a, c, e) reflected a distance of less than 1m between the GI and the edge of the road, leaving no space for placing instruments; these sites are referred to as 'close-road' (Fig 1g). The remaining sites with measurement locations behind and in front of the GI (Figs 1b, d, f) had more than 2m in distance from the edge of the road to GI, leaving enough space to place the instrument in front of GI; these sites are referred to as 'away-road' (Figs 1f). Henceforth, the terms 'close-road' and 'away-road' are used to define the 'clear area and behind (CB)' and 'in front and behind (IB)' sites, respectively (Table 2).

All six measurement locations were near to residential areas containing two-storey buildings or sections of surrounding public parks, falling under typical open road environments. In particular, sites H_{CB} (Aldershot-Hedge) and T_{CB} (Aldershot-Tree) are along the same road and are approximately 200m away from each other (Fig 1a, c). These sites are situated in a residential area with double-storey houses on either side of the two-lane road. Similarly, T_{IB} (Sutherland-Tree) and TH_{IB} (Sutherland-GI) sites are 100m apart from each other and are next to a recreational park near the two-lane road (Fig. 1d, e). H_{IB} (Stoke Road-Hedge) site is near to a children's play area, adjacent to a two-lane street passing through a residential area (Fig 1b). TH_{IB} at Shalford is next to a public park and a busy two-lane road is close to the vegetation barrier. Average traffic volume and direction of roads at each site were counted (Table 2).

2.2 Data collection

We simultaneously monitored PM_1, $PM_{2.5}$, PM_{10}, PNC and BC behind and in front of or adjacent to the GI. Two GRIMM aerosol monitors (model EDM 107 and 11-C) measured PM_1, $PM_{2.5}$ and PM_{10}. Both instruments measured PM mass concentrations in 31 different size channels at a resolution of 6 seconds. These instruments have been widely used for PM concentration measurements (Azarmi and Kumar, 2016; Rivas et al., 2017; Viippola et al., 2018). The mass of bulk particles was collected on a PTFE filter in the GRIMM monitors, which were analysed using SEM-EDS to allow chemical and morphological exploration (Azarmi and Kumar, 2016; Rivas et al., 2017) (Section 2.4). Three filter papers were collected from behind and in front of or adjacent clear area of the GI and filter papers were changed after 10 days of measurements (80 to 100 hours of sampling). Two P-TRAK 8525 (TSI Inc.) were employed to measure PNC in the size range of 0.02 to 1μm. Studies on the impacts of barriers in open road environments and personal exposure studies have used these instruments (Baldauf et al., 2008; Rivas et al., 2017). Both P-TRAKs measured PNC every 6 seconds. BC concentrations were collected using two portable MicroAeth AE51 (Aethlabs), which is widely employed for personal exposure assessments (Rivas et al., 2017). Attenuation in BC data generated due to instrumental optical and electronic noise is rectified by post-processing the data with the Optimised Noise-reduction Averaging algorithm (ONA; Hagler, et al. 2011). Filter papers of microaeths were changed every 20 hours of sampling and sampling rate was set to 100 ml m^{-1} to reduce the effect of filter loading. The time base was set to 10 seconds. Later, all measured data were combined by averaging over 1 minute. Breaks of 10 to 30 minutes were taken for changing the batteries of the GRIMM monitors and re-filling the alcohol in the P-TRAK wicks. Leaf area index (LAI) is a dimensionless metric of leaf area per unit ground area m^2/m^2. It is estimated from changes in photosynthetically active radiation passing through overlaying foliage by the handheld ceptometer Accu-PAR LP80. LAI measurements were carried out at the beginning and end of sampling at each location and used to determine the leaf area density (LAD).

Meteorological conditions (i.e., wind direction, wind speed, temperature and relative humidity) during monitoring periods were obtained from the nearest UK weather station, located in Farnborough (~10km northwest of Guildford). Previous studies have utilised data from this meteorological station (Al-Dabbous and Kumar, 2014; Goel and Kumar, 2016). In addition, micrometeorological conditions were collected by portable weather station Kestrel 4500 at a 1.5m height above the road level. Local and reference wind direction bias was checked and provided in Supplementary Information, SI, Figs S1 and S2. Traffic counting was performed for 20 minutes in every hour of monitoring during each day of measurement, with the help of the SMART Traffic Counter App developed by the University of Wollongong, Australia. Later, the collected traffic counts of 20 minutes were extrapolated to generate an hourly average, as shown in Table 2.

Sampling location had two sets of instruments (includes GRIMM, P-TRAK, and MicroAeth) mounted on a tripod stand at a 1.5m height to sample air from a typical breathing height. One tripod was kept behind the GI at all sites and the other one was placed in an adjacent clear area at sites H_{CB}, T_{CB} and TH_{CB} and behind the GI at sites H_{IB}, T_{IB} and TH_{IB}. The portable weather station was always attached to the tripod in the adjacent clear area or in front of the GI. The campaign collected 5 days of monitoring data per site, making a total of 30 days. Each day, measurement started and ended around 08.00 h and 18.00 h (local time), respectively, producing 8 to 10 hours of high-resolution data daily. Field measurements were not carried out on rainy days in order to ensure the safety of the instruments.

2.3 Data processing

All the data were cleaned and processed using R Statistical software (v3.0.2, R Core Team, 2016). Statistical analyses were performed using the *openair* package (Carslaw and Ropkins, 2012). In order to investigate the influence of wind direction on pollution exposure, the data was divided based on the wind flow direction with respect to street and GI alignment. The dataset was divided into three wind direction sectors: 'along-road' (parallel to road), 'cross-road' (wind from road to GI), and 'cross-vegetation' (wind from GI to the road), as demonstrated in Fig 2 by the yellow (along-road), green (cross-vegetation) and blue (cross-road) shaded areas. Along-road wind condition included two 60^0 circular sectors (30^0 either side of parallel axis), with their centres passing through the parallel axis of GI/road (Fig 2a). This represents parallel wind conditions and includes wind coming from either end of GI. The centers of cross-road and cross-vegetation wind sectors passed through the perpendicular axis of GI and road, and consisted of circular sections with an angle of 120^0 on both sides of GI, as shown in Fig 2a. Both wind sectors represent perpendicular wind directions.

2.4 SEM and EDS analysis

The bulk particles were collected on 47mm PTFE filter using the GRIMM 107 and GRIMM 11-C, representing measurements behind and in front of or adjacent to the GI. Each location had three filter paper samples. For analysing morphology and the elemental composition of individual particles, samples were made by cutting a 1 cm × 1 cm area from all filter papers, at the Micro-Structural Studies Unit of the University of Surrey, UK. These samples were mounted on aluminum studs and carbon coated. Prepared specimens were analysed by a Scanning Electron Microscope, JEOL SEM (model JSM-7100F, Japan) equipped with an energy dispersive X-ray spectrometer. The SEM has a spatial resolution of 1.2 nm at 30 kV and 3.0 nm at 1 kV. SEM was operated at an acceleration voltage of 10kv, with a working distance of 10mm under vacuum conditions. As the filter paper substrate is made of carbon and fluorine, their presence was removed from the particle spectrum in SEM-EDS analysis. Backscattering electron (BSE) detectors were employed to identify particles with higher atomic number elements. This forms a contrasting image, with bright white particles of higher atomic number elements and a black background consisting of other particles of lower atomic number elements and filter paper (Fig 3). Images with white particles were analysed with Pathfinder software from Thermo-Fisher in automated mode. Ten random images were taken from each sample of behind GI measurement point and clear-area/in front of GI location making 60 micrographs in total. Around 20000 random particles from these images were analysed and categorised based on the elemental composition (Section 3.5).

2.5 Quality control

Two sets of portable high-end instruments were used for the monitoring of BC (microAeth AE51), PM (GRIMM 107 and 11-C), and PNC (P-TRAK 8525). All the instruments were calibrated prior to fieldwork. One in each pair of the instruments was calibrated later than the other, and was considered as a base instrument to harmonise the data. For quality assurance of the data collected by instruments, we implemented the following quality control strategy as also used by previous studies (Lin et al. 2016; Brantley et al., 2014). We co-located both sets of instruments side-by-side for at least 30 minutes prior to start and after the GI monitoring campaigns each day. On some days, we carried out this co-location exercise in the middle of the monitoring period, when instruments were restarted after a battery change. The total period of co-location data accounted for ~10% of total field campaign data, enabling us to inter-compare results from two identical instruments and assess the relative difference. All our instruments performed well against their counterpart and obtained a good agreement (Fig 4). We obtained (i) a minimum R^2 value of 0.85 for BC measurements by microAeths; (ii) GRIMMs showed R^2 values of 0.87, 0.93, and 0.88 for PM_{10}, $PM_{2.5}$ and PM_1, respectively; and (iii) P-TRAKs showed the highest R^2 value (0.97) among all instruments (Fig 4). Even though these correlations were satisfactory, a slight difference in instrument results can be expected. To remove this discrepancy, we corrected the data obtained from one of the instruments using the equations derived from the scatter plots (Fig 4). These correlations account for various factors, including the different field measurement conditions and possible differences in meteorological conditions, such as high and low ambient temperature and relative humidity.

3. Results and Discussion

3.1 Overall pollutant concentration changes with different GI

Figure 5 shows the summary of pollutant concentration changes at six monitoring sites. Table 3 shows the summary statistics of recorded measurements. At most sites, PNC concentrations behind the GI were found to be modestly lower than clear (–2%) or in front of (–3%) GI, except in the cases of T_{CB} and TH_{CB} in close-road sites. The maximum improvement in PNC concentrations behind GI was observed with hedges (H_{IB} and H_{CB}) in both close-road and away-road sites, with –30% and –9%, respectively. The reductions seen from H_{IB} and the combination of trees and hedges were comparable to those reported previously by Al-Dabbous and Kumar (2014) and Hagler et al. (2012). At close-road sites, BC concentrations behind the GI were found to be slightly higher than in the adjacent clear area, except for the tree and hedge configuration (TH_{CB}; 4%), which was similar to those reported by Brantley et al. (2014). The H_{CB} site emerged as the worst scenario among close-road sites (15%). Conversely, away-road sites displayed higher BC concentration reductions in the range of –43 to –63%, with lowest at H_{IB} and highest at TH_{IB}. Percentage changes in BC concentrations (ΔBC) were relatively high when compared with the other pollutants investigated in this study (Table 3).

Similar to ΔBC, ΔPM_{10} behind the GI also exhibited a similar trend in both close-road and away-road sites, but the magnitude of ΔPM_{10} was lower compared to ΔBC. The highest improvement in ΔPM_{10} was observed for trees with hedge in away-road (TH_{IB}; –24%) and close-road (TH_{CB}; –7%) sites, respectively. The highest deterioration (22%) in ΔPM_{10} behind GI was noticed in the hedge only (H_{CB}) scenario of close-road sites. Almost all previous away-road studies (Chen et al., 2016; Islam et al., 2012; Shan et al., 2007; Tiwary et al., 2008) have reported a high reduction of PM_{10} compared to close-road (Chen et al., 2015; Viippola et al., 2018).

The percentage changes in $PM_{2.5}$ concentrations ($\Delta PM_{2.5}$) were the lowest in magnitude compared to other pollutants. $\Delta PM_{2.5}$ behind the GI matched the trend of ΔBC and ΔPM_{10} in close-road and reversed concentration change profile for ΔBC and ΔPM_{10} at away-road sites. Here, a maximum improvement of 8% was recorded in trees with hedges (TH_{CB}) in close-road sites and an increase in $\Delta PM_{2.5}$ for ~22% is reported with hedge only (H_{CB}). Meanwhile, the maximum reduction of $PM_{2.5}$ was displayed by the hedge only scenario (H_{IB}; –14%) and the least was displayed by trees with hedges (TH_{IB}; –8%) at away-road sites. Past studies reported inconclusive results while investigating $PM_{2.5}$ concentration behind GI regardless of adopted locations for comparison (Table 1).

Improvement in PM_1 concentration behind GI was observed in most of the investigated scenarios, except hedge only ($H_{CB;}$ 1%) in close-road sites. ΔPM_1 followed the same trend as $\Delta PM_{2.5}$. Hedge only (H_{IB}; 25%) and tress with hedges (TH_{CB} 19%) recorded the highest PM_1

concentration reductions behind the GI in away-road and close-road sites, respectively. Such variations in ΔPM_1 behind GI at the tree only (T_{CB}) site was nominal.

In summary, the H_{IB} site presented better improvement in air quality behind GI across measured pollutants, followed by TH_{IB} in away-road sites, whereas TH_{CB} displayed improvement in air quality in close-road sites. H_{CB} and T_{CB} sites presented a deterioration of air quality behind GI under close-road conditions. Although, the magnitude of increase in pollutant concentration changes were less than 7%, expect PM_{10} concentrations (22%) and BC (15%) at hedges only (H_{CB}) site. Since the comparisons were made between the pair of GI types in investigated under away-road and close-road sites, the higher concentration reduction in former case could be due to the build-up of pollutants concentrations in-front of GI compared to the latter case where measurement points were at the same distance (Fig 1). Usually, a higher reduction of pollutant concentration is expected with an increase in LAD. However, we found an opposite trend for H_{CB} (LAD = 5.5 m^2m^{-3}) and H_{IB} (LAD = 2.4 m^2m^{-3}), where elevated concentrations were observed for nearly all of the pollutants. These concentrations could be due to a relatively low height of H_{CB} (<1m) that is insufficient to create a barrier effect. Similarly, past investigations have reported mixed results of pollutant concentrations behind trees that emerged from a lack of barrier effect at breathing height and lower density (Brantley et al., 2014; Chen et al., 2016; Hagler et al., 2012; Viippola et al., 2018; Yli-Pelkonen et al., 2017). In addition, major reasons for higher pollutant concentrations behind trees ($T_{CB;}$ single tree row) compared with T_{IB} (multiple tree rows, up to 4) was due to the difference in thickness of tree rows and lower canopy to ground distance. The physical structures of TH_{CB} (naturally occurring) and TH_{IB} were comparable but TH_{IB} site had a well-maintained hedge in front of the tree row. This configuration was revealed to be the most effective tree and hedge combination for achieving a maximum reduction in pollutant concentrations.

The above finding highlights the importance of GI configurations in reducing exposure concentrations for various pollutants. Among all pollutants, the highest relative differences were seen for BC and PNC (rapid decay) and the least for $PM_{2.5}$ (gradual decay). Finally, we observed that hedges, and the combination of trees with hedges, provided the better reduction potential.

3.2 Effects on wind direction

In order to understand the influence of wind direction on concentrations behind the GI, we separated the wind conditions into three main categories: *along-road*, *cross-road* and *cross-vegetation* (Fig 2), as explained in Section 2.3. For some sites, we did not have enough data points available; for example, during cross-road winds at TH_{IB} and cross-vegetation winds at both the T_{CB} and H_{IB} sites (Table S2). ΔPNC in three investigated wind directions were lower than that of ΔBC and were similar to ΔPM_1. *Along-road* wind conditions resulted in a maximum reduction between wind categories. H_{IB} and H_{CB} in both *close-road* and *away-road* sites showed the highest reduction in ΔPNC of –30% and –50%, respectively (Fig 6). In *cross-road* conditions, H_{IB} displayed a maximum reduction (–30%) in PNC, followed by T_{CB} (–13%) and H_{CB} (–12%). The highest deterioration in PNC among all wind conditions was reported during *cross-road* winds, although less than 5% at sites T_{CB} and TH_{CB} (Table S2). Lowest ΔPNC were observed with *cross-vegetation* compared to other wind directions and the highest improvement in PNC concentration was noticed for TH_{IB} (–13%; Table S2). Al-Dabbous and Kumar (2014) investigated hedges similar to H_{IB} and reported –77%, and –37% reductions in ΔPNC concentrations in *along-road* and *cross-road* wind directions, respectively. H_{IB} displayed –50% and –30% reductions in ΔPNC concentrations with corresponding wind conditions. ΔPNC in *cross-road* wind conditions were comparable and *along-road* wind direction displayed higher ΔPNC than *cross-road* winds in both studies.

Highest relative changes between measurements taken behind GI and in front of GI/clear areas were observed with BC compared other investigated pollutants. Furthermore, the maximum percentage differences in BC were comparable across different wind directions (Fig 6). A relatively small (<6%) increase in ΔBC was observed at TH_{CB} site during *along-road* wind directions opposed to a reduction of –7.8% reported by Brantley et al. (2014). Conversely, improvement in BC concentrations ranged from –49% (H_{IB}) to –65% (TH_{IB}) at away-road sites (Table.S2). During *cross-road* winds, all sites showed an improvement in BC concentrations behind the GI except for H_{CB} (–23%). The T_{CB} and TH_{CB} close-road sites saw a –11% improvement, in line with the ~12% reported by Brantley et al. (2014) for GI with similar LAI values. T_{IB} showed the highest change (52%) in ΔBC concentrations among studied sites (Table.S2). BC is a good traffic emission tracer, indicating no deterioration in air quality behind GI during *cross-vegetation* wind directions. Moreover, ΔBC under *cross-vegetation* winds ranged from –12% (T_{IB}) to –61% (TH_{IB}). In the case of trees with hedges (TH_{IB} and TH_{CB}), the maximum reduction in BC concentration was found in away-road (–65%) and close-road (–43%), respectively.

The influences of GI on ΔPM_{10} under different wind conditions were similar except at the H_{CB} and T_{CB} sites (Fig 6). During *along-road* winds, the majority of cases displayed improvements of about –12 to –16% in ΔPM_{10} behind GI, while the H_{CB} and T_{CB} sites displayed reductions of just 6% and 8%, respectively. The highest reductions in ΔPM_{10} were recorded at TH_{CB} (–16%) sites in near-road conditions and at H_{IB} (–14%) in away-road conditions. Under *cross-road* wind conditions, only H_{CB} showed an increase in PM_{10} concentrations (22%) and all other improvements in ΔPM_{10} ranged from –2% (T_{CB}) to –15% (H_{IB}) (Table S2). During *cross-vegetation* winds, all sites exhibited a reduction in PM_{10} except H_{CB}, with an increase of 21% behind the hedge. Maximum improvement in PM_{10} concentrations was presented by trees with hedges in both close-road and away-road cases, providing further evidence of GI removing PM_{10} effectively in open road conditions.

$\Delta PM_{2.5}$ concentrations were lower than all other measured pollutants in this study (Fig 6). H_{CB} and T_{CB} sites showed deterioration in $PM_{2.5}$ concentration behind the GI for all wind directions. In *along-road* wind direction, the highest improvements were revealed by TH_{CB} (–17%) at close-road sites and T_{IB} (–14%) in away-road sites. During *cross-road* winds, H_{IB} (–17%) displayed maximum reductions. All close-road sites exhibited positive differences in $PM_{2.5}$, ranging from 2% to 7% in the *cross-vegetation* wind category (Table S2). Past studies investigating different GI (Brantley et al., 2014;Chen et al., 2016; Tong et al., 2015; Viippola et al., 2018; Morakinyo et al., 2016) recorded a mixed (increase or decrease) trend for $PM_{2.5}$ (Table 1), as was also noticed in this study. Hedges and trees with hedges were effective in reducing $PM_{2.5}$. As discussed in Section 3.1 and highlighted by previous studies (Abhijith et al., 2017; Baldauf, 2017), GI dimensions such as the height and thickness could be primary reasons for increases in different pollutant concentrations behind H_{CB} and T_{CB} compared to T_{IB} and H_{IB} with similar LAD.

In most of the wind categories, influences on ΔPM_1 were positive (Fig 6). The magnitude of differences was similar to PNC and higher than PM_{10} and $PM_{2.5}$ (Table S2). For example, during *along-road* winds, highest improvements were noticed at close-road site TH_{CB} (–29%) and T_{IB} (–18%) in away-road sites, similar to $PM_{2.5}$ variation. During the *cross-road* winds, TH_{CB} (–14%) in close-road sites and H_{IB} (–31%) in away-road sites reported the highest reductions in PM_1. No increase in PM_1 concentrations behind GI was noticed under *cross-road* winds. Lastly, *cross-vegetation* winds showed improvement in PM_1 concentrations, except at H_{CB} site (Fig 6).

In summary, the magnitude of percentage differences followed the following trend:

$\Delta PM_{2.5}<\Delta PM_{10}<\Delta PM_1<\Delta PNC<\Delta BC$. Generally, higher percentage changes were reported during *along-road* winds due to sweeping effects, followed by upwind areas of *cross-road* and *cross-vegetation* winds. TH_{CB} in close-road sites and H_{IB} in away-road sites reported the highest reduction in pollutant concentrations, mainly during *along-road* and *cross-road* wind conditions. These observations clearly indicate that due consideration of local wind directions during the urban planning of new built-up areas could help to reduce exposure of roadside users. In *cross-vegetation* winds, TH_{CB} and TH_{IB} cases showed a high percentage reduction among all GI. H_{CB} showed an increase in all pollutants (mainly PMs) except BC in *cross-vegetation* winds, indicating upwind sources of pollutants other than the road (maybe from houses as traffic correlated BC is absent). Similarly, increases in other cross-vegetation cases pointed towards emissions from background residential areas since no increase in BC concentrations were noticed. Most of the increases in pollutant concentrations behind GI were found in H_{CB} and T_{CB} sites and had a strong correlation with their physical dimensions. Hedge height at H_{CB} was lower (~1 m) and T_{CB} has a single tree row with no buffer by its trunk at measurement height, assisting in the accumulation of pollutants and failing to create a significant barrier effect (Hagler et al., 2012).

3.3 The effect of vegetation density on changes in relative concentrations

In order to assess the effect of vegetation density on percentage differences in pollutant concentration behind the GI, the correlation coefficient (R^2) between LAD and relative pollutant concentration were drawn (SI Fig S3). As mentioned in Section 3.2, a full dataset was not available for *cross-road* and *cross-vegetation* wind directions and such scenarios were therefore excluded in this analysis. While analysing the overall data, we observed R^2 well below 0.8 at close-road and away-road sites for more than half of the cases and were considered as insignificant (Fig 7). Strong correlations of LAD were only found with ΔPNC in all investigated cases. Similarly, ΔPM_{10} at close-road sites and ΔPM_1 and $\Delta PM_{2.5}$ at away-road sites exhibited a significant correlation with LAD (R^2 >0.9). These observations indicated an increase in pollutant concentration reduction behind the GI with an increase in LAD, supporting our previous observations (Abhijith et al., 2017). This analysis of experimental observations testified the outcomes of a modelling study by Tong et al. (2016) on the relationship between ΔPNC behind GI and LAD. Interestingly, ΔPM_{10} showed an increase in concentration behind the GI with an increase in LAD, requiring further investigations to provide a clear explanation for this trend.

3.4 Influence of GI on PM fractions

Figure 8 shows the differences in the percentage of PM fractions behind GI and in front of or in a clear area adjacent to GI for the studied GI configurations. At most GI sites, PM_1 fraction of fine particles dominated the total PM fractions in adjacent clear area and in front of GI compared to PM_1 behind the GI. This indicated the presence of fresh emissions from traffic in front of GI and adjacent clear area, and a reduction of corresponding PM_1 fine fraction behind GI after passing through the barrier. While considering overall PM fractions in hedges, both H_{CB} and H_{IB} displayed a reduction in fine particles (PM_1 and $PM_{1-2.5}$) behind GI, with H_{CB} showing a relatively higher reduction between them (Fig 8). Hedges with leaves close to ground-level assisted in reducing the traffic-originated fine fraction of PM (PM_1 and $PM_{1-2.5}$) by providing a barrier effect and surfaces for deposition at breathing level. This PM removal mechanism of hedges was pronounced when emissions were transported from the road to GI in a *cross-road* wind direction, and the higher reduction was observed in corresponding wind conditions (Fig 8). No significant changes in any PM fractions were observed during *cross-vegetation* winds. Both tree-only sites (i.e., T_{IB} and T_{CB}) displayed no significant changes in PM fractions under overall and studied wind directions. This was expected as there was only a main trunk or stem of the tree between the tree canopy base and ground-level, resulting in an absence of a barrier effect and surfaces for deposition in the breathing zone. The changes in

PM fractions behind GI in a combination of trees with hedges (TH_{IB} and TH_{CB}) were influenced by either hedges or trees depending on wind directions. During *along-road* winds, fine (PM_1 and $PM_{1-2.5}$) and coarse ($PM_{2.5-10}$) particle fractions displayed no considerable variations behind the GI at all sites. Parallel air flow along GI limited penetration of particles into the body of GI, thereby minimising the effect of GI on PM fractions. During *cross-wind* conditions, TH_{CB} sites showed a reduction in fine particle fractions behind the GI, indicating filtration of these traffic-originated particles by the hedges at breathing height, similar to hedge-only sites. While in *cross-vegetation* winds, TH_{IB} and TH_{CB} resulted in a large reduction of coarse particles behind the GI when compared with in the front of or adjacent clear area to the GI. This could be attributed to fresh emissions from neighbouring houses or other activities as stated in Section 3.2.

Figure 9 shows a comparison of ratios of $PM_1/PM_{2.5}$ and $PM_{2.5}/PM_{10}$ at all the sites. The sites displayed dominance of PM_1 particles in $PM_{2.5}$ as seen from the $PM_1/PM_{2.5}$ being >0.6. All sites had a slight difference between values of $PM_1/PM_{2.5}$ ratios behind GI and those in front of or in the clear area adjacent to GI. Conversely, ratios of $PM_{2.5}/PM_{10}$ recorded a significant reduction of $PM_{2.5}$ behind the GI when compared with areas in front of or adjacent to GI ($PM_{2.5}/PM_{10}$ behind GI $<PM_{2.5}/PM_{10}$ in front/clear area). This demonstrated a lower concentration of fine particles behind GI when compared with in front of or adjacent to GI, and hence provides further evidence of fine particle removal through deposition and the barrier effect.

3.5 Elemental composition of individual particles

A total of 10491 particles from the front/clear areas and 9819 particles from behind GI were identified for analysis. We classified the particles based on their elemental composition as natural, vehicle, salt, and unclassified. Figure 11 shows the images of representative particles such as NaCl, pollens and carbon soot and sulphur rich particles found on the PTFE filter papers from behind and in the front/clear area. We identified 4564 and 4908 natural particles on the filter papers from the in-front/clear area and behind GI locations, respectively. The particles in the natural category were dominated by commonly found earth elements, such as Si, Ca, Al, Mg, Fe, K, S and P. An individual particle was listed as natural where the sum of the percentage weight of its constituent elements exceeded 70%. Previous studies have identified these elements arising from sources such as road dust and soil (Jancsek-Turóczi et al., 2013; Panda and Shiva Nagendra, 2018). Under the vehicle category, 1419 individual particles were classified from the in-front/clear area filter paper and, of those, 903 particles were iron and its oxides, usually found in exhaust and brake and tyre wear from road vehicles (Weerakkody et al., 2018). By comparison, 725 particles were classified under the vehicle category from the behind GI filter paper. Among identified particles, iron oxides and other metals (Ba, Cr, V, Ti) constituted 406 and 319 respectively. Vehicle particles have either 70% of iron and its oxides or at least 60% of elemental weight compositions of Ba, Cr, Mn, Cu, V and Ti. Vehicle category elements (Fe Ba, Cr, Mn, Cu, V and Ti) are tracers of vehicular exhaust and non-exhaust emissions (González et al., 2017; Mazziotti Tagliani et al., 2017; Weerakkody et al., 2018), of which, Ba, Zn, and Cu have been identified as brake lining emissions in previous studies (Hays et al., 2011; Moreno et al., 2015). Salt is used on the roads for gritting and NaCl crystals were clearly noticeable as perfect cuboids in the collected particles. In salt particles, 80% of weight consisted of sodium (Na) and chlorine (Cl). As opposed to particles of other classifications, almost double the number of salt (NaCl) particles were found behind GI (1068) compared to in front of or in clear areas adjacent to GI (593).The remaining particles were agglomerates of above-mentioned particles and their elemental composition was evenly distributed among them. A total of 3915 from the in-front/adjacent clear areas and 3118 from behind GI were listed in the unclassified category.

Overall, mean values of percentage weight elemental compositions of particles in the same classification from behind GI and in front of or clear area adjacent to GI were comparable. For example, the NaCl category accounted for 45% of Cl and 35% of Na at both locations. Iron-rich particles of the vehicle category consisted of Fe (57% behind, 54% in clear area/in-front) and oxygen (17% behind, 18% in clear area/in-front) dominated both locations (SI Table 3). Other particles in the vehicle category were dominated by Ba, followed by Mn, Cr, V, and Ti. Although the percentage difference of vehicle group between behind and in front of or clear area adjacent to vegetation were smaller, these elements are toxic even in lower concentrations. When comparing identified particles from behind GI with those from the other monitoring locations, natural (+7%) and NaCl (+5%) particles were higher behind GI than in front of or in a clear area adjacent to GI (Fig 11). Conversely, a significantly lower percentage (–7%) of vehicle particles were found behind GI than in the other monitoring locations (Fig 11). In terms of particle count, 725 particles were from vehicular origin out of a total of 9819 particles collected from behind the GI, as opposed to 1419 from 10491 particles collected from in front of or in a clear area adjacent to GI. This difference indicates the positive effect of GI in reducing traffic-related emission exposure. In addition, the fraction of the unclassified group, which includes some traffic-originated particles, were found to be lower by about 5% behind the GI when compared with the other monitoring locations, further substantiating the potential for removal of harmful particles by GI through deposition.

4. Summary, Conclusions and Future Work

This experimental investigation measured and compared different pollutant (BC, PNC, PM_{10}, $PM_{2.5}$, and PM_1) concentrations from behind GI with those from a clear area adjacent to or in front of GI. We evaluated three GI types (hedges, trees, and a combination of hedges and trees) in close-road and away-road environments and under *along-road* (parallel to the road), *cross-road* (perpendicular to the road, from the road to GI) and *cross-vegetation* (opposite to cross-road) wind conditions. We also investigated the fractional composition of PM and the elemental composition behind the GI to ascertain possible GI induced alternation.

The following conclusions were drawn:

- The overall data, without segregating by ambient wind directions, suggested that hedge-only (H_{IB}) scenarios presented better improvement in air quality behind GI across all measured pollutants, at both away-road and close-road sites. Trees with hedges (TH_{IB}; TH_{CB}) scenarios were found to be the second most effective configuration type. Tree-only scenarios did not show any positive influences on the measured concentrations. The use of hedges or a combination of hedges and trees, therefore, emerged as favourable options for the reduction of pollutant concentrations behind vegetation.

- When comparing concentration changes among pollutants, the highest relative differences were observed for BC, followed by PNC and $PM_{1,}$ which was expected due to their modest background concentrations when compared with $PM_{10.}$ The lowest relative differences were observed for $PM_{2.5}$ behind the GI.

- The assessments based on wind directions revealed a maximum reduction in pollutant concentration during *along-road* wind conditions, followed by *cross-road* wind conditions, showing up to a 52, 30, 15, 17 and 31% reduction for BC, PNC, PM_{10}, $PM_{2.5}$ and PM_1, respectively.

- The analysis of vegetation density indicated higher relative pollutant reductions with an increase in LAD. ΔPNC showed a significant correlation with LAD. GI dimensions such as thickness and height had an important role in lowering pollutant concentrations behind GI. For example, single tree rows (thinner; T_{CB}) showed a deterioration of air quality compared to multiple tree rows (thicker; T_{IB}), even though both had similar LAD.

Similarly, a lower hedge height (H_{CB}) was revealed to be ineffective in reducing pollutant concentrations when compared to a taller hedge (H_{IB}).

- No change in PM fractional composition was observed behind the GI in the presence of trees. However, both the hedge-only and trees with hedges scenarios resulted in lower fractions of sub-micron particles. The SEM single particle analysis led to a reduction in traffic-related particles (vehicle; 7%) in samples taken from behind the GI compared to those taken in front of or clear area adjacent to GI. In addition, naturally occurring particles were dominant behind the GI (7%) and agglomerates of particles originating from natural and vehicular sources were lower (–5%) behind the GI. The evidence from the SEM single particle elemental investigation demonstrated a reduction of harmful traffic-related particles by GI via deposition and enhanced dispersion.

We compared a pair of the same GI types under two distinct (in-front vs behind in away-road environments, and clear area versus behind in close-road environments) scenarios that provided scientific evidence for the efficacy of GI for air pollution exposure reduction in real-world cases. The close-road cases revealed a difference in concentration changes due to additional accumulation of pollutants in front of vegetation. On the contrary, the away-road cases provided insight into additional dilution effects of pollutants due to an increased distance from the road. While our ingenious portable set-up allowed monitoring at desired locations, it limited long-term unattended measurements that are recommended to allow the covering of different seasons and the construction of a database that can help to formulate guidelines for GI design and implementation.

5. Acknowledgements

This work is supported by the iSCAPE (Improving Smart Control of Air Pollution in Europe) project, which is funded by the European Community's H2020 Programme (H2020-

SC5-04-2015) under the Grant Agreement No. 689954. We thank Aakash C. Rai, Prashant Rajput, Imogen Wadlow, Rana Moustafa and Swathi Nimje for their kind help during our monitoring campaigns. We also thank Justine Fuller and Gary Durant from the Guildford Borough Council for their help in accessing the sites for monitoring campaigns. We express our sincere gratitude to Dave Jones for helping and facilitating SEM analysis at Micro-Structural Studies Unit of the University of Surrey.

6. References

Abhijith, K.V., Kumar, P., Gallagher, J., McNabola, A., Baldauf, R., Pilla, F., Broderick, B., Di Sabatino, S., Pulvirenti, B., 2017. Air pollution abatement performances of green infrastructure in open road and built-up street canyon environments – A review. Atmos. Environ. 162, 71–86.

Agency, European Environment, 2015. Air quality in Europe — 2015 report, Report. doi:10.2800/62459

Al-Dabbous, A.N., Kumar, P., 2014. The influence of roadside vegetation barriers on airborne nanoparticles and pedestrians exposure under varying wind conditions. Atmos. Environ. 90, 113–124.

Azarmi, F., Kumar, P., 2016. Ambient exposure to coarse and fine particle emissions from building demolition. Atmos. Environ. 137, 62–79.

Baldauf, R., 2017. Roadside vegetation design characteristics that can improve local, near-road air quality. Transp. Res. Part D Transp. Environ. 52, 354–361.

Baldauf, R., Thoma, E., Khlystov, A., Isakov, V., Bowker, G., Long, T., Snow, R., 2008. Impacts of noise barriers on near-road air quality. Atmos. Environ. 42, 7502–7507.

Baldauf, R.W., Heist, D., Isakov, V., Perry, S., Hagler, G.S.W., Kimbrough, S., Shores, R., Black, K., Brixey, L., 2013. Air quality variability near a highway in a complex urban environment. Atmos. Environ. 64, 169–178.

Batterman, S., 2013. The Near-Road Ambient Monitoring Network and Exposure Estimates for Health Studies. EM (Pittsburgh. Pa). 2013, 24–30.

Batterman, S., Chambliss, S., Isakov, V., 2014. Spatial resolution requirements for traffic-related air pollutant exposure evaluations. Atmos. Environ. 94, 518–528.

Brantley, H.L., Hagler, G.S.W., J. Deshmukh, P., Baldauf, R.W., 2014. Field assessment of the effects of roadside vegetation on near-road black carbon and particulate matter. Sci. Total

Environ. 468–469, 120–129.
Brook, R.D., Rajagopalan, S., Pope, C.A., Brook, J.R., Bhatnagar, A., Diez-Roux, A. V., Holguin, F., Hong, Y., Luepker, R. V., Mittleman, M.A., Peters, A., Siscovick, D., Smith, S.C., Whitsel, L., Kaufman, J.D., 2010. Particulate matter air pollution and cardiovascular disease: An update to the scientific statement from the american heart association. Circulation 121, 2331–2378.
Cahill, T. a., Barnes, D.E., Withycombe, E., Watnik, M., 2011. Very Fine and Ultrafine Metals and Ischemic Heart Disease in the California Central Valley 2: 1974–1991. Aerosol Sci. Technol. 45, 1135–1142.
Carrier, M., Apparicio, P., Séguin, A.M., Crouse, D., 2014a. The application of three methods to measure the statistical association between different social groups and the concentration of air pollutants in Montreal: A case of environmental equity. Transp. Res. Part D Transp. Environ. 30, 38–52.
Carrier, M., Apparicio, P., Séguin, A.M., Crouse, D., 2014b. Ambient air pollution concentration in montreal and environmental equity: Are children at risk at school? Case Stud. Transp. Policy 2, 61–69.
Chen, L., Liu, C., Zou, R., Yang, M., Zhang, Z., 2016. Experimental examination of effectiveness of vegetation as bio-filter of particulate matters in the urban environment. Environ. Pollut. 208, 198–208.
Chen, X., Pei, T., Zhou, Z., Teng, M., He, L., Luo, M., Liu, X., 2015. Efficiency differences of roadside greenbelts with three configurations in removing coarse particles (PM10): A street scale investigation in Wuhan, China. Urban For. Urban Green. 14, 354–360.
Clark, N.A., Demers, P.A., Karr, C.J., Koehoorn, M., Lencar, C., Tamburic, L., Brauer, M., 2010. Effect of early life exposure to air pollution on development of childhood asthma. Environ. Health Perspect. 118, 284–290.
EPA, 2016. Health Impacts of Near Roadway Air Pollution and Mitigation Strategies Different types of roadways.
European Environment Agency, 2015. State and Outlook 2015 the European Environment. doi:10.2800/944899
European Environment Agency, 2013. Air quality in Europe—2013 Report: EEA report no 9/2013, European Union. doi:10.2800/92843
Evans, K.A., Halterman, J.S., Hopke, P.K., Fagnano, M., Rich, D.Q., 2014. Increased ultrafine particles and carbon monoxide concentrations are associated with asthma exacerbation among urban children. Environ. Res. 129, 11–19.

Fantozzi, F., Monaci, F., Blanusa, T., Bargagli, R., 2015. Spatio-temporal variations of ozone and nitrogen dioxide concentrations under urban trees and in a nearby open area. Urban Clim. 12, 119–127.

Gallagher, J., Baldauf, R., Fuller, C.H., Kumar, P., Gill, L.W., McNabola, A., 2015. Passive methods for improving air quality in the built environment: A review of porous and solid barriers. Atmos. Environ. 120, 61–70.

Goel, A., Kumar, P., 2016. Vertical and horizontal variability in airborne nanoparticles and their exposure around signalised traffic intersections. Environ. Pollut. 214, 54–69.

González, L.T., Longoria Rodríguez, F.E., Sánchez-Domínguez, M., Cavazos, A., Leyva-Porras, C., Silva-Vidaurri, L.G., Askar, K.A., Kharissov, B.I., Villarreal Chiu, J.F., Alfaro Barbosa, J.M., 2017. Determination of trace metals in TSP and PM2.5materials collected in the Metropolitan Area of Monterrey, Mexico: A characterization study by XPS, ICP-AES and SEM-EDS. Atmos. Res. 196, 8–22.

Grundström, M., Pleijel, H., 2014. Limited effect of urban tree vegetation on NO2 and O3 concentrations near a traffic route. Environ. Pollut. 189, 73–76.

Guerreiro, C., Gonzalez Ortiz, A., de Leeuw, F., Viana, M., Horalek, J., 2016. Air quality in Europe — 2016 report.

Hagler, G.S.W., Lin, M.Y., Khlystov, A., Baldauf, R.W., Isakov, V., Faircloth, J., Jackson, L.E., 2012. Field investigation of roadside vegetative and structural barrier impact on near-road ultrafine particle concentrations under a variety of wind conditions. Sci. Total Environ. 419, 7–15.

Hays, M.D., Cho, S.H., Baldauf, R., Schauer, J.J., Shafer, M., 2011. Particle size distributions of metal and non-metal elements in an urban near-highway environment. Atmos. Environ. 45, 925–934.

HEI, 2010. Traffic-related air pollution: a critical review of the literature on emissions, exposure, and health effects. Heal. Eff. Inst. Special Re, 1–386.

Islam, M.N., Rahman, K.S., Bahar, M.M., Habib, M.A., Ando, K., Hattori, N., 2012. Pollution attenuation by roadside greenbelt in and around urban areas. Urban For. Urban Green. 11, 460–464.

Jancsek-Turóczi, B., Hoffer, A., Nyírö-Kósa, I., Gelencsér, A., 2013. Sampling and characterization of resuspended and respirable road dust. J. Aerosol Sci. 65, 69–76.

Karner, A.A., Eisinger, D.S., Niemeier, D.E.B.A., 2010. Near-Roadway Air Quality : Synthesizing the Findings from Real-World Data 44, 5334–5344.

Kim, J.J., Smorodinsky, S., Lipsett, M., Singer, B.C., Hodgson, A.T., Ostro, B., 2004. Traffic-

related air pollution near busy roads: The East Bay Children's Respiratory Health Study. Am. J. Respir. Crit. Care Med. 170, 520–526.
Klingberg, J., Broberg, M., Strandberg, B., Thorsson, P., Pleijel, H., 2017. Influence of urban vegetation on air pollution and noise exposure – A case study in Gothenburg, Sweden. Sci. Total Environ. 599–600, 1728–1739.
Kumar, P., Patton, A.P., Durant, J.L., Frey, H.C., 2018a. A review of factors impacting exposure to PM2.5, ultrafine particles and black carbon in Asian transport microenvironments. Atmos. Environ. 187, 301–316.
Kumar, P., Rivas, I., Sachdeva, L., 2017. Exposure of in-pram babies to airborne particles during morning drop-in and afternoon pick-up of school children. Environ. Pollut. 224, 407–420.
Kumar, P., Rivas, I., Singh, A.P., Ganesh, V.J., Ananya, M., Frey, H.C., 2018b. Dynamics of coarse and fine particle exposure in transport microenvironments. Clim. Atmos. Sci. 11, 1–12.
Laumbach, R.J., Kipen, H.M., 2012. Respiratory health effects of air pollution: Update on biomass smoke and traffic pollution. J. Allergy Clin. Immunol. 129, 3–11.
Lee, E.S., Ranasinghe, D.R., Ahangar, F.E., Amini, S., Mara, S., Choi, W., Paulson, S., Zhu, Y., 2018. Field evaluation of vegetation and noise barriers for mitigation of near-freeway air pollution under variable wind conditions. Atmos. Environ. 175, 92–99.
Lin, M.Y., Hagler, G., Baldauf, R., Isakov, V., Lin, H.Y., Khlystov, A., 2016. The effects of vegetation barriers on near-road ultrafine particle number and carbon monoxide concentrations. Sci. Total Environ. 553, 372–379.
Mazziotti Tagliani, S., Carnevale, M., Armiento, G., Montereali, M.R., Nardi, E., Inglessis, M., Sacco, F., Palleschi, S., Rossi, B., Silvestroni, L., Gianfagna, A., 2017. Content, mineral allocation and leaching behavior of heavy metals in urban PM2.5. Atmos. Environ. 153, 47–60.
Michelle Wilhelm, Jo Kay Ghosh, Jason Su, Myles Cockburn, Michael Jerrett, B.R., 2012. Traffic-Related Air Toxics and Term Low Birth Weight in Los Angeles County, California. Environ. Health Perspect. 132–138.
Morakinyo, T.E., Lam, Y.F., Hao, S., 2016. Evaluating the role of green infrastructures on near-road pollutant dispersion and removal: Modelling and measurement. J. Environ. Manage. 182, 595–605.
Moreno, T., Martins, V., Querol, X., Jones, T., BéruBé, K., Minguillón, M.C., Amato, F., Capdevila, M., de Miguel, E., Centelles, S., Gibbons, W., 2015. A new look at inhalable

metalliferous airborne particles on rail subway platforms. Sci. Total Environ. 505, 367–375.

Padró-Martínez, L.T., Patton, A.P., Trull, J.B., Zamore, W., Brugge, D., Durant, J.L., 2012. Mobile monitoring of particle number concentration and other traffic-related air pollutants in a near-highway neighborhood over the course of a year. Atmos. Environ. 61, 253–264.

Panda, S., Shiva Nagendra, S.M., 2018. Chemical and morphological characterization of respirable suspended particulate matter (PM10) and associated heath risk at a critically polluted industrial cluster. Atmos. Pollut. Res. 1–13.

Pasquier, A., André, M., 2017. Considering criteria related to spatial variabilities for the assessment of air pollution from traffic. Transp. Res. Procedia 25, 3358–3373.

Patton, A.P., Perkins, J., Zamore, W., Levy, J.I., Brugge, D., Durant, J.L., 2014. Spatial and temporal differences in traffic-related air pollution in three urban neighborhoods near an interstate highway. Atmos. Environ. 99, 309–321.

Rivas, I., Kumar, P., Hagen-Zanker, A., 2017. Exposure to air pollutants during commuting in London: Are there inequalities among different socio-economic groups? Environ. Int. 1–15.

Shan, Y., Jingping, C., Liping, C., Zhemin, S., Xiaodong, Z., Dan, W., Wenhua, W., 2007. Effects of vegetation status in urban green spaces on particle removal in a street canyon atmosphere. Acta Ecol. Sin. 27, 4590–4595.

Sharma, A., Kumar, P., 2018. A review of factors surrounding the air pollution exposure to in-pram babies and mitigation strategies. Environ. Int. 120, 262–278.

Steffens, J.T., Heist, D.K., Perry, S.G., Isakov, V., Baldauf, R.W., Zhang, K.M., 2014. Effects of roadway configurations on near-road air quality and the implications on roadway designs. Atmos. Environ. 94, 74–85.

Surrey-i, 2015. Census key statistics (Key demographics , age , gender , ethnicity , religion , disability , health and carers), Guildford Local Authority in Surrey 25–27.

Tian, N., Xue, J., Barzyk, T.M., 2013. Evaluating socioeconomic and racial differences in traffic-related metrics in the United States using a GIS approach. J Expo. Sci Env. Epidemiol 23, 215–222.

Tiwary, A., Reff, A., Colls, J.J., 2008. Collection of ambient particulate matter by porous vegetation barriers: Sampling and characterization methods. J. Aerosol Sci. 39, 40–47.

Tong, Z., Baldauf, R.W., Isakov, V., Deshmukh, P., Max Zhang, K., 2016. Roadside vegetation barrier designs to mitigate near-road air pollution impacts. Sci. Total Environ. 541, 920–927.

Tong, Z., Whitlow, T.H., Macrae, P.F., Landers, A.J., Harada, Y., 2015. Quantifying the effect of vegetation on near-road air quality using brief campaigns. Environ. Pollut. 201, 141–149.

United Nations, 2014. World Urbanization Prospects 2014. Demogr. Res. 32. doi:(ST/ESA/SER.A/366)

Viippola, V., Whitlow, T.H., Zhao, W., Yli-Pelkonen, V., Mikola, J., Pouyat, R., Setälä, H., 2018. The effects of trees on air pollutant levels in peri-urban near-road environments. Urban For. Urban Green. 30, 62–71.

Volk, H.E., Hertz-Picciotto, I., Delwiche, L., Lurmann, F., McConnell, R., 2011. Residential proximity to freeways and autism in the CHARGE study. Environ. Health Perspect. 119, 873–877.

Weerakkody, U., Dover, J.W., Mitchell, P., Reiling, K., 2018. Quantification of the traffic-generated particulate matter capture by plant species in a living wall and evaluation of the important leaf characteristics. Sci. Total Environ. 635, 1012–1024.

Wilker, E.H., Mostofsky, E., Lue, S.H., Gold, D., Schwartz, J., Wellenius, G.A., Mittleman, M.A., 2013. Residential proximity to high-traffic roadways and poststroke mortality. J. Stroke Cerebrovasc. Dis. 22, e366–e372.

Yin, S., Shen, Z., Zhou, P., Zou, X., Che, S., Wang, W., 2011. Quantifying air pollution attenuation within urban parks: An experimental approach in Shanghai, China. Environ. Pollut. 159, 2155–2163.

Yli-Pelkonen, V., Viippola, V., Kotze, D.J., Setälä, H., 2017. Greenbelts do not reduce NO2concentrations in near-road environments. Urban Clim. 21, 306–317.

List of Figures

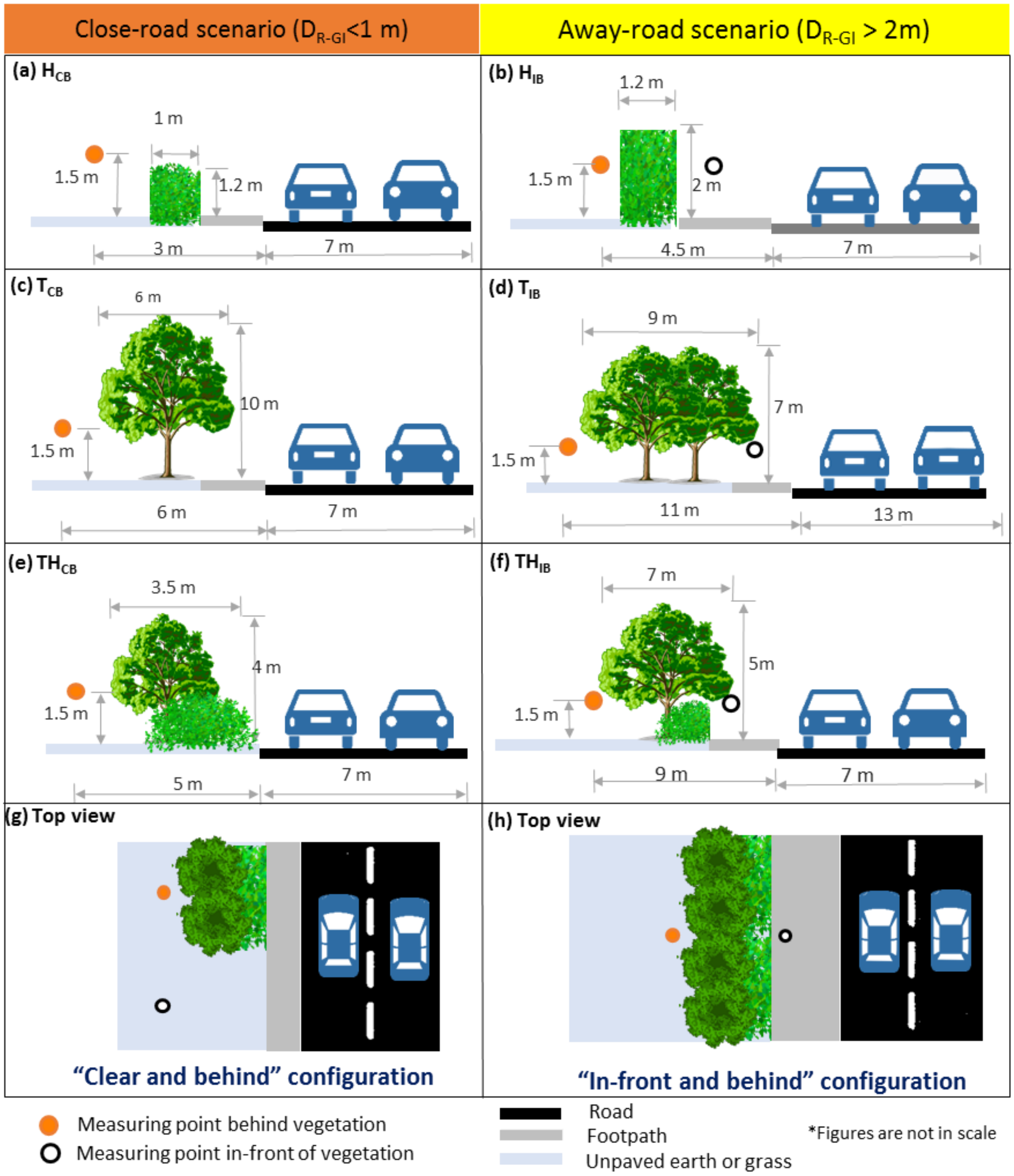

Figure 1. Schematic representation of six monitoring locations with the type of GI and road details. The orange circle and black ring denote measurement points behind and in front of the GI, respectively. $D_{R\text{-}GI}$ refers to the distance between the road and the GI types.

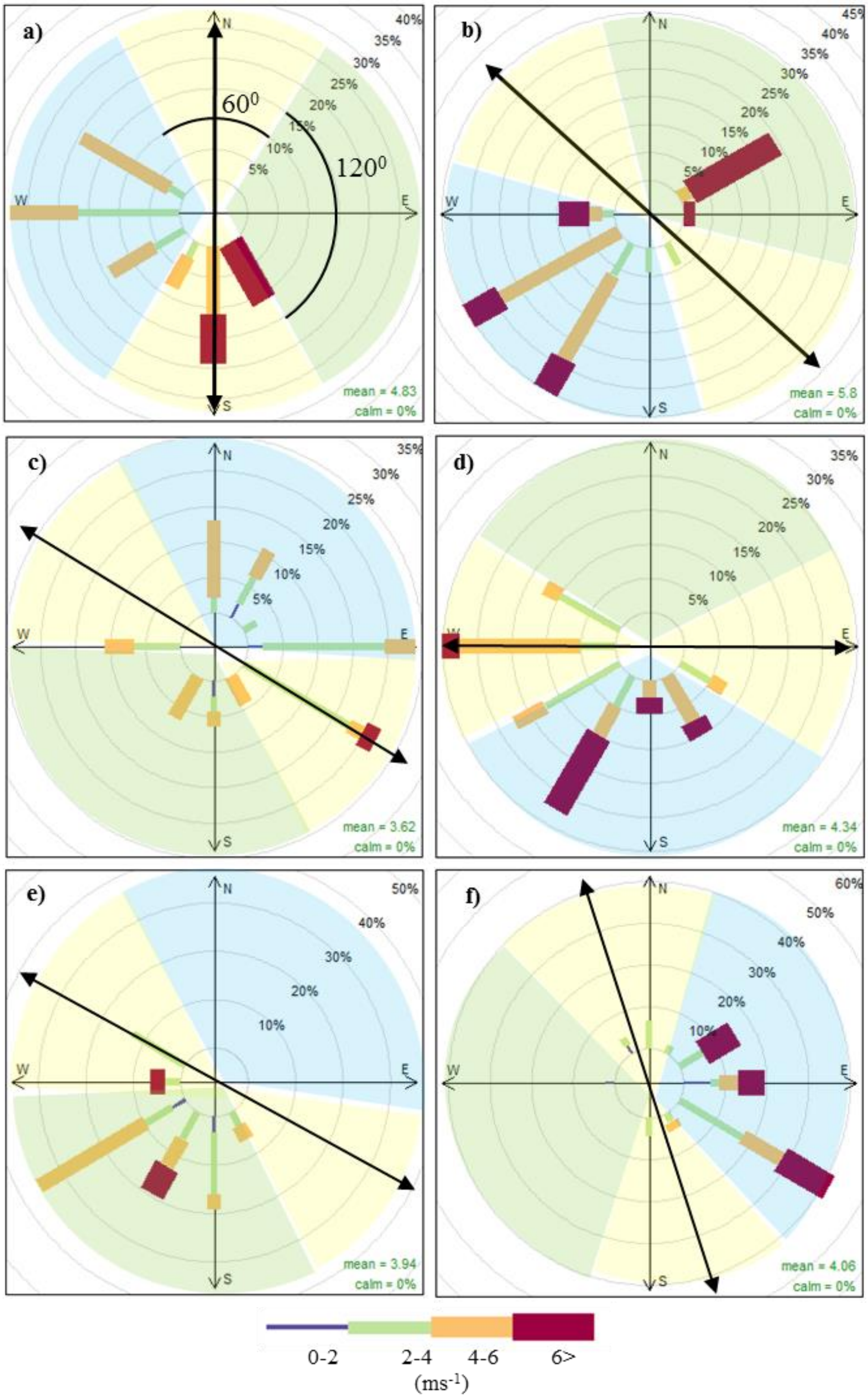

Figure 2. Windrose diagrams at each of the monitoring locations (a) H_{IB}, (b) H_{CB}, (c) T_{IB}, (d) T_{CB}, (e) TH_{IB}, and (f) TH_{CB} over the entire sampling duration. The road is marked as a black coloured arrow. The colour shading denotes wind direction conditions with respect to street axis: cross-road (blue), along-road (yellow), and cross-vegetation (green).

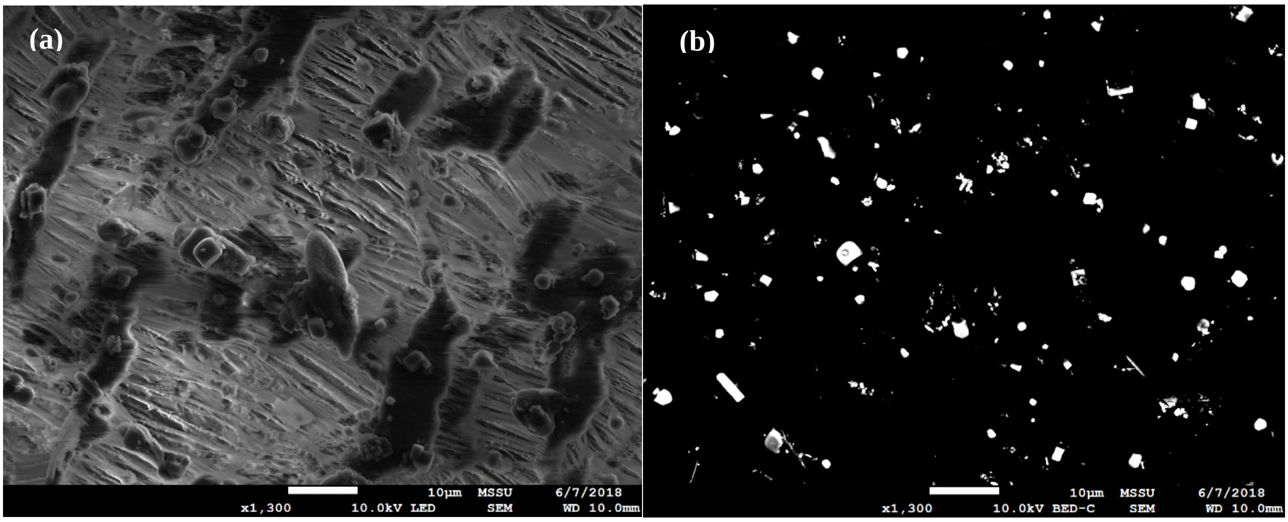

Figure 3. SEM image of particle deposited on filter paper showing: (a) visible light, and (b) backscattering electron which highlights particles with a higher atomic number.

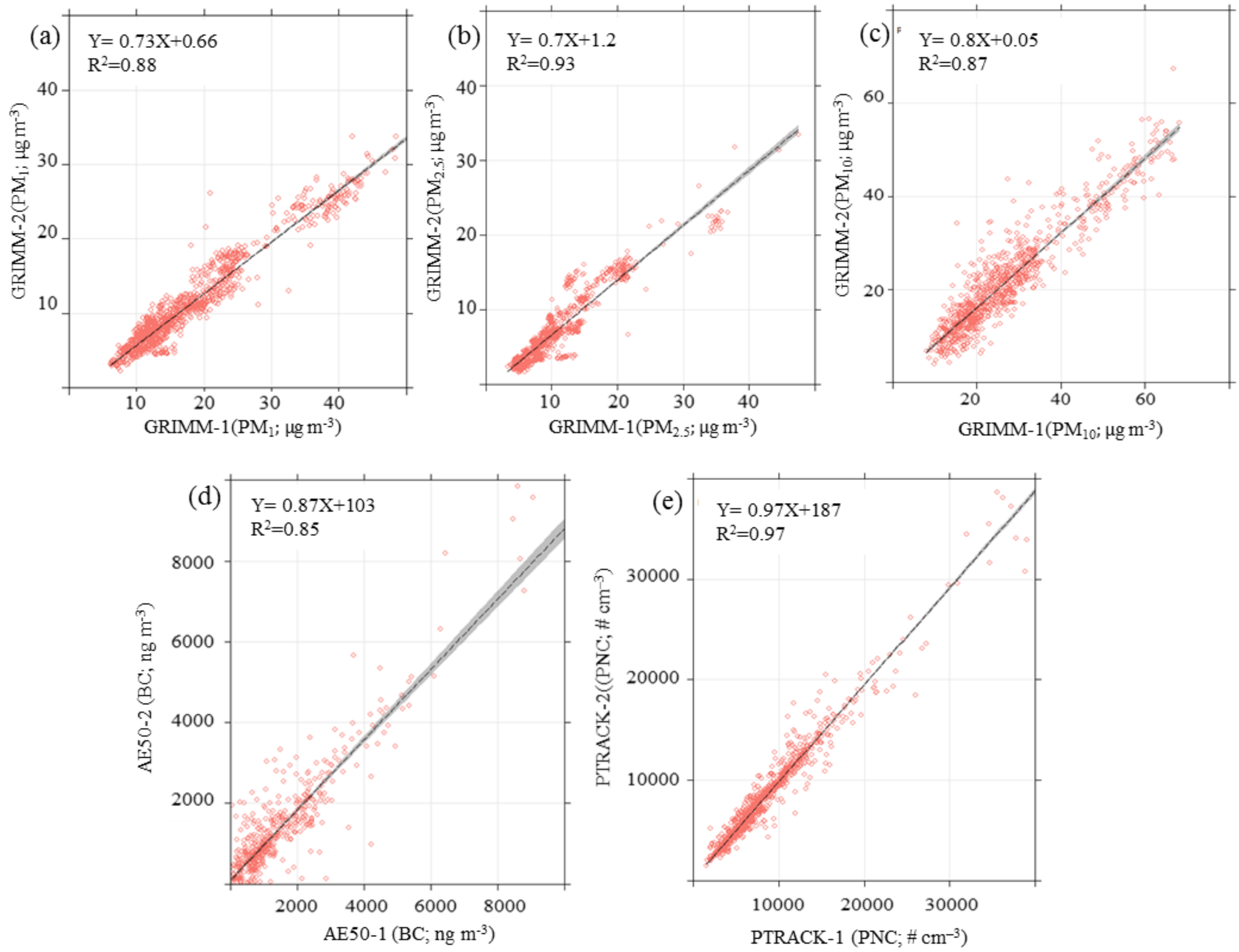

Figure 4. Scatterplots of co-located instruments for: (a) PM_1, (b) $PM_{2.5}$, (c) PM_{10} measurements by GRIMM 11-C (x-axis) and GRIMM 107 (y-axis), (d) BC measurements by microAeth AE51, and (e) PNC measurements by both P-TRAK models.

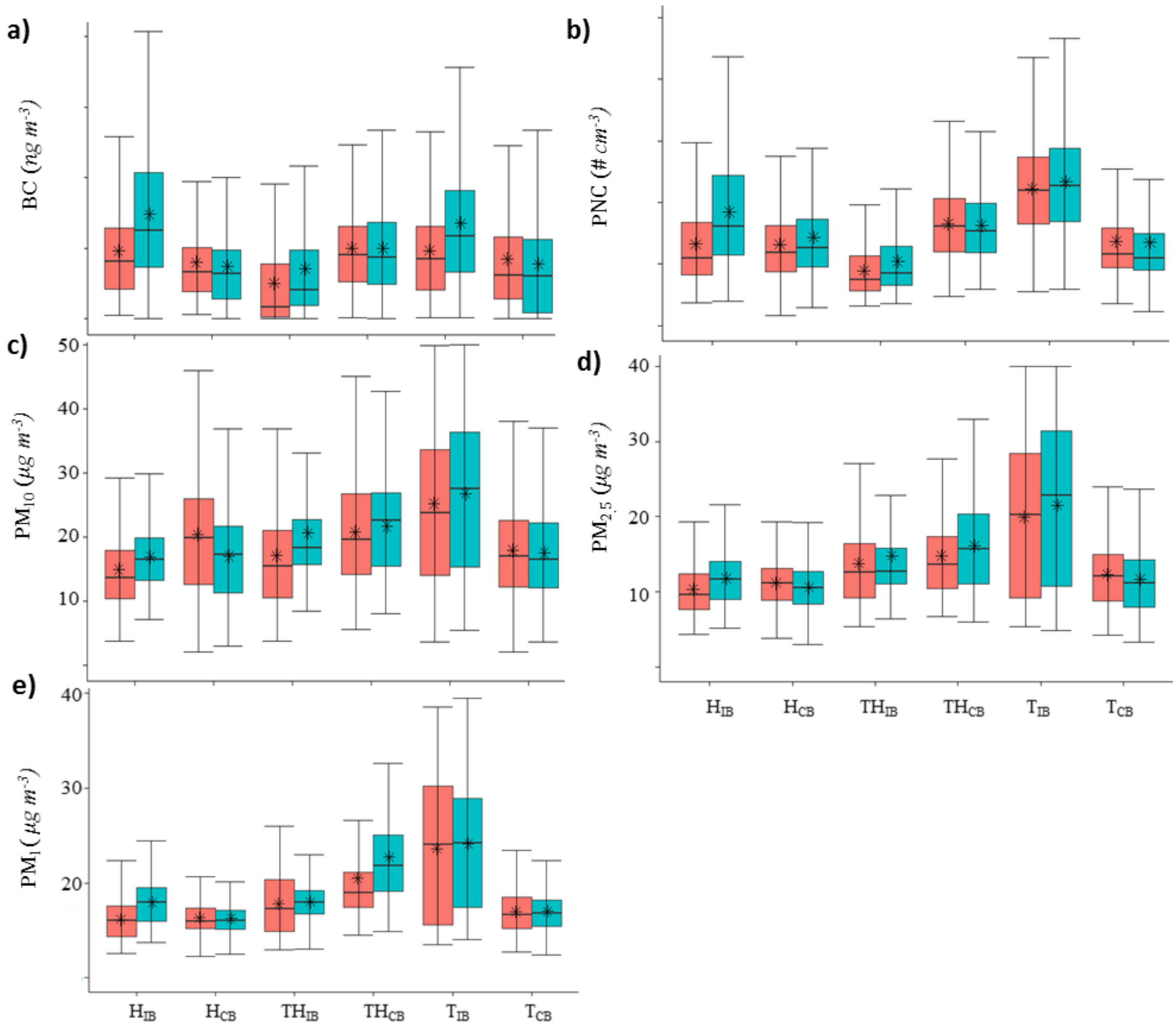

Figure 5. Boxplots of pollutant concentration behind (red) and in-front/clear (green) measurement points at six monitoring sites for (a) BC, (b) PNC, (c) PM_{10}, (d) $PM_{2.5}$, and (e) PM_1 concentrations; mean values are shown as star notation.

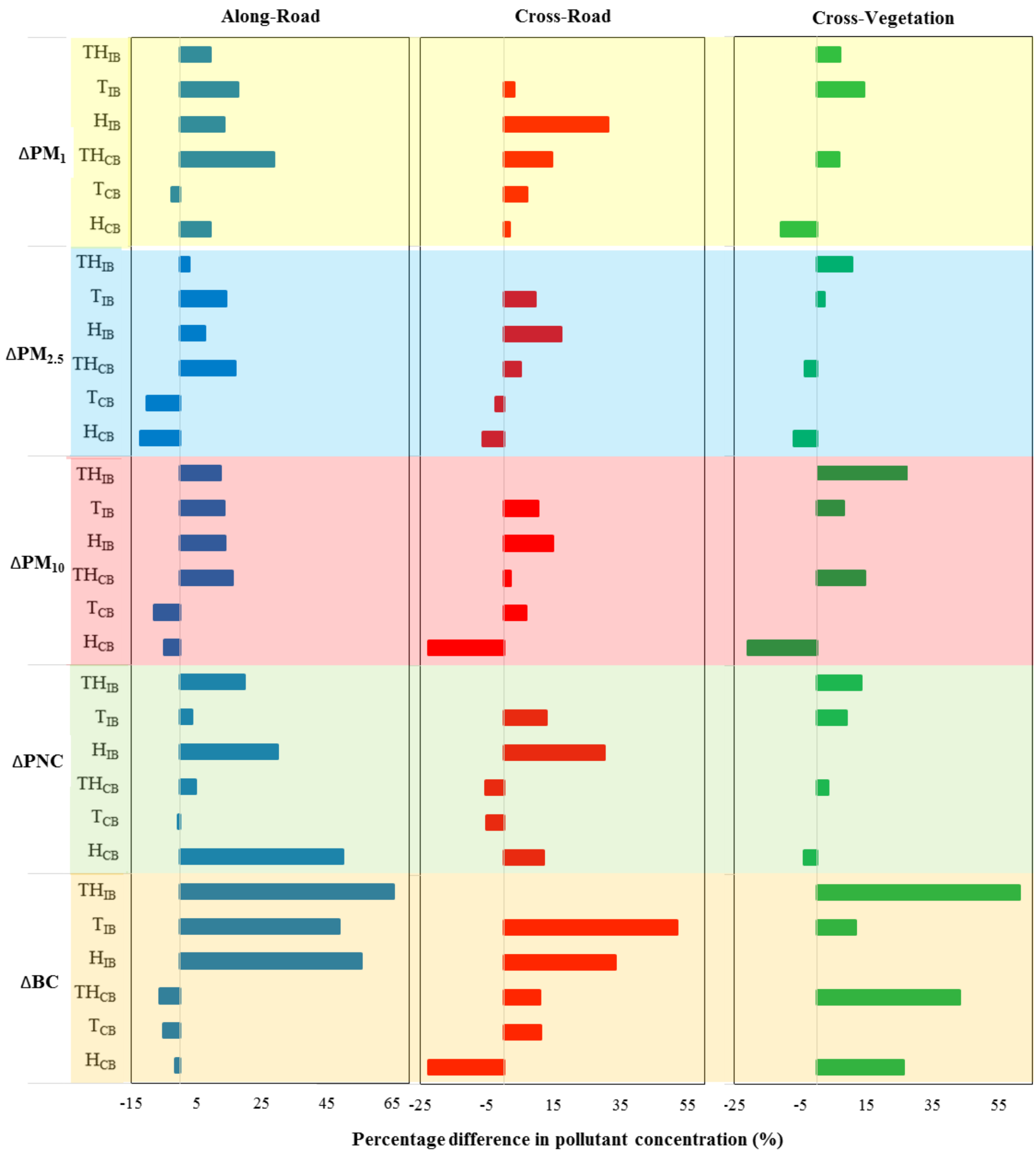

Figure 6. The percentage differences in various pollutants under *along-road*, *cross-road* and *cross-vegetation* wind conditions. The positive and negative differences indicated reduced and increased concentrations behind the GI at the close- and away-road sites.

Pollutants	Overall		Along-road wind direction	
	CB	**IB**	**CB**	**IB**
BC	0.70	0.12	**0.86**	0.02
PNC	**0.99**	**0.99**	**0.99**	**0.83**
PM_{10}	**0.84**	0.01	0.08	0.25
$PM_{2.5}$	0.15	**0.94**	0.20	0.11
PM_1	0.24	**0.91**	0.00	0.05

Figure 7. Correlation of percentage difference in pollutant concentrations with respect to LAD of GI in *behind vs clear* and *behind vs in front* scenarios. Red colour indicates an increase in pollutant concentration with increase in LAD and green colour vice-versa. The grey colour denotes insignificant R^2 values.

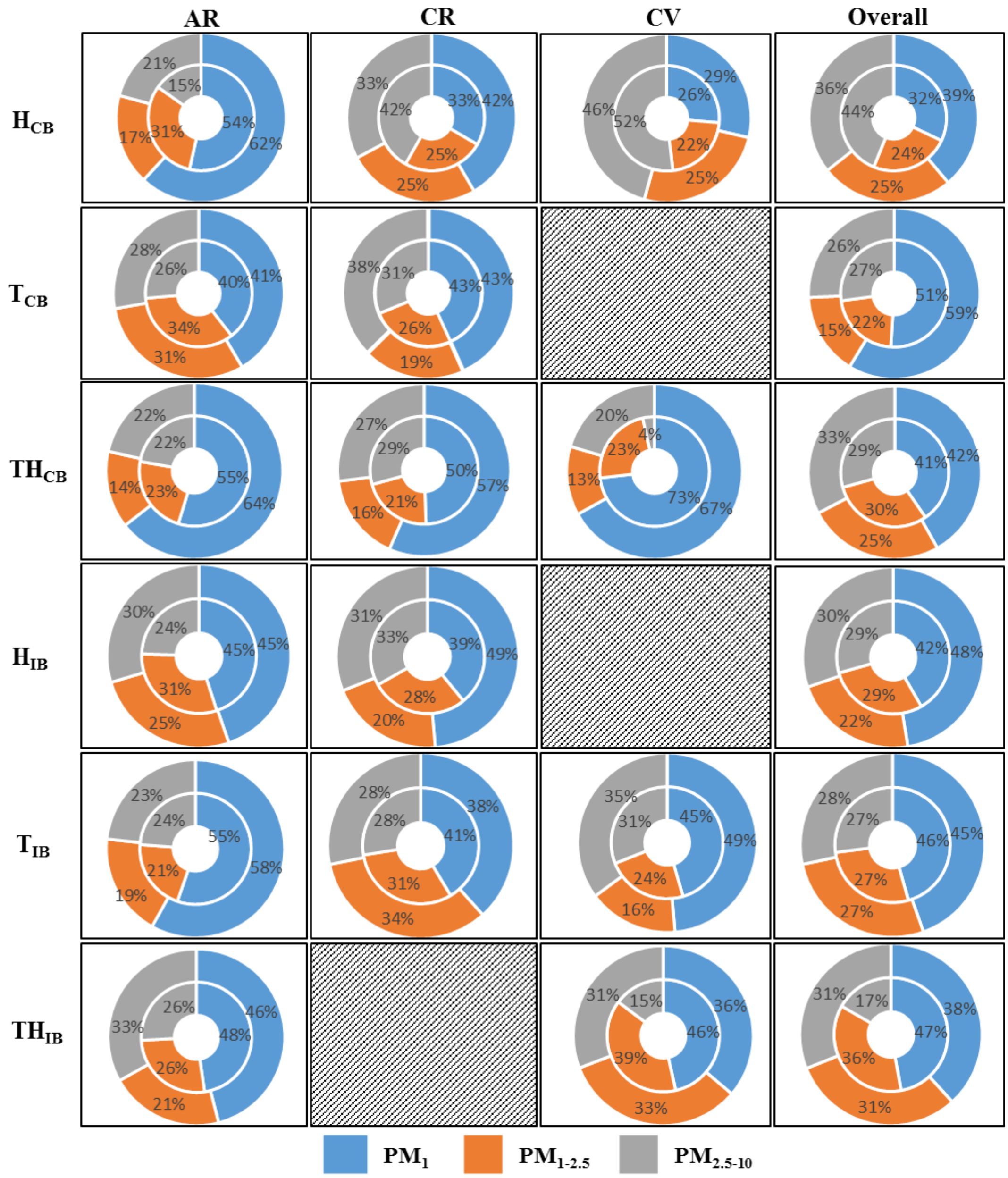

Figure 8. The fraction of various PM types at all the six sites under different wind directions. The inner circle shows PM fractions behind the GI; the outer circle shows PM fractions in-front/clear areas. Blue, orange and grey colours denote PM_1, $PM_{1-2.5}$ and $PM_{2.5-10}$, respectively. Line shading represents a lack of data available in particular situations.

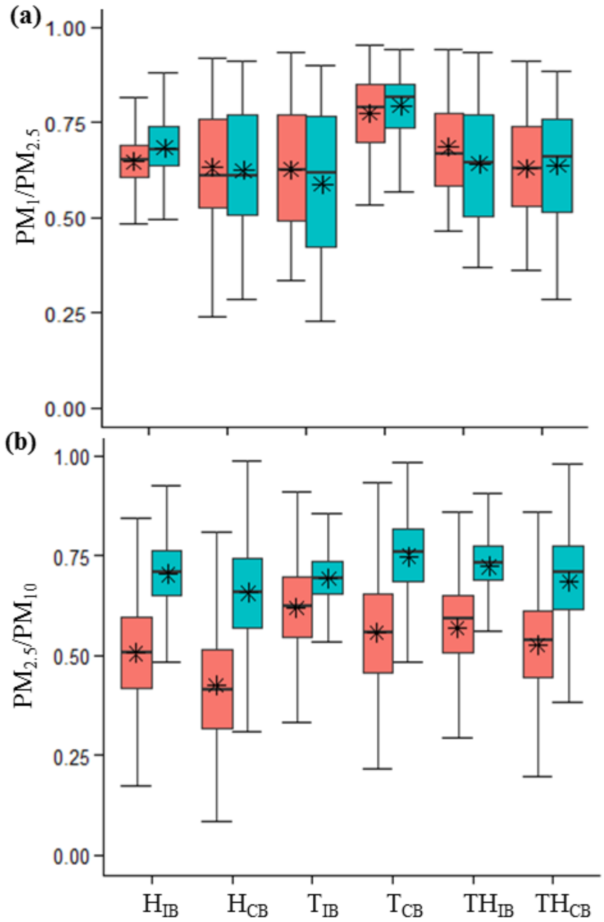

Figure 9. The ratios of (a) $PM_1/PM_{2.5}$ and (b) $PM_{2.5}/PM_{10}$ at the studied sites.

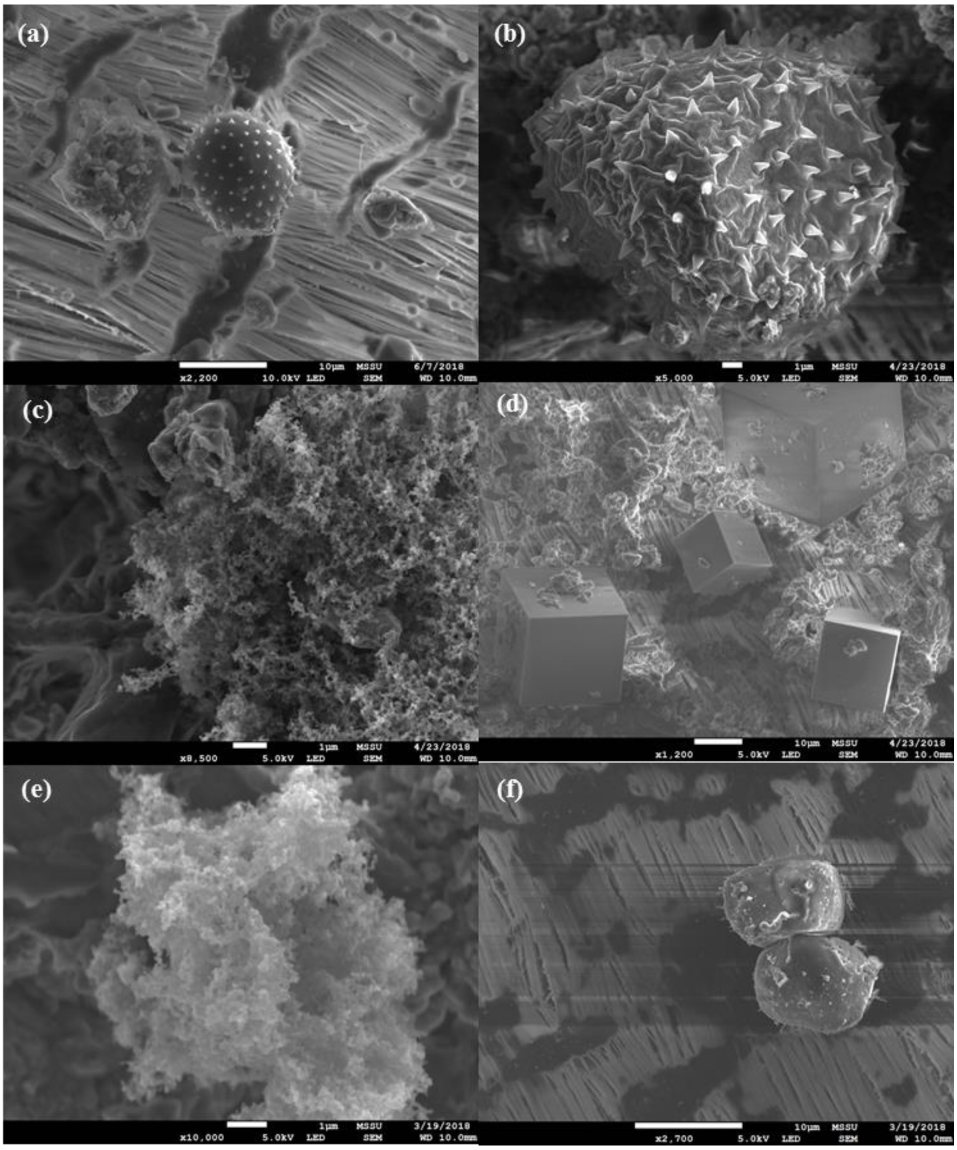

Figure 10. SEM micrographs showing some of the identified particles on the PTFE filter paper and their elemental composition. (a) Pollen form plants (×2200), (b) pollen (×5000), (c) particle with high sulphur (×8500), (d) salt particles (×1200), (e) carbon soot (×10000), and (f) particle with high carbon content (×2700).

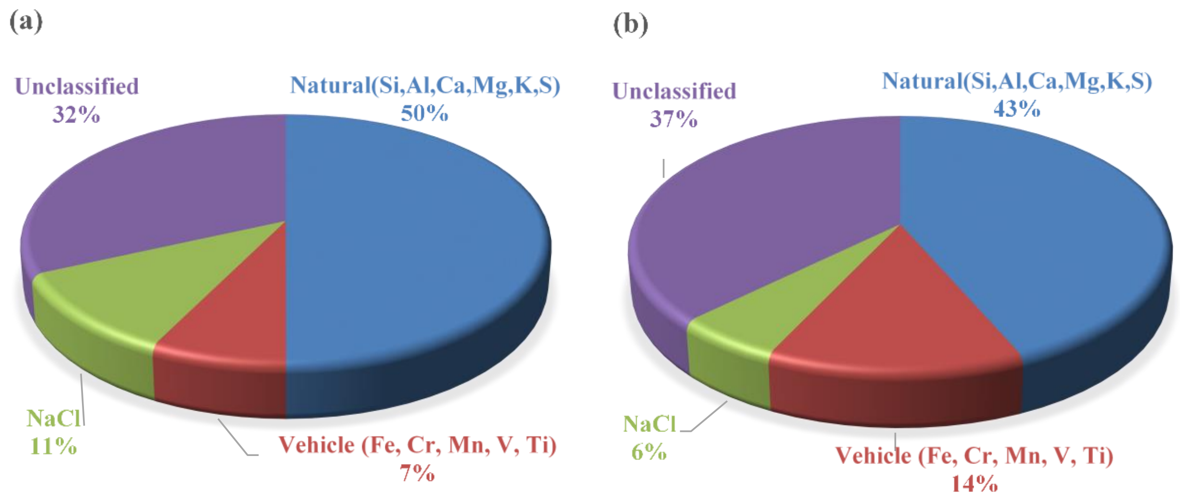

Figure 11. Percentage of samples identified in each elemental composition group in total particles on the PTFE filters (a) behind, and (b) in-front/clear of GI.

List of Tables

Table 1. Summary of relevant research studies undertaken on air pollution reduction by the GI.

Pollutant and concentration decay trend with distance	GI type	Changes in pollutant concentration behind GI	References
No Trend: PM_{10}, TSP	Hedge	Reduction of 45-60% Reduction of 7-9% Reduction of 34%	Chen et al. (2016) Chen et al. 2015) Tiwary et al. (2008)
	Tree	Mixed (higher and lower) Reduction of 30-60% Reduction of 5-35% Large reduction	Brantley et al. (2014) Chen et al. (2016) Yin et al. (2011) Viippola et al. (2018)
	Combination of Tree and hedge	Reduction 10-70% Reduction of 7-15% Reduction of 12-65% Reduction of 30-65%	Chen et al. (2016) Chen et al. (2015) Islam et al. (2012) Shan et al. (2007)
Gradual: $PM_{2.5}$	Hedge	Reduction 5-35%	Chen et al. (2016)
	Tree	No Significant difference Mixed -20 to 20% Higher behind trees 10% Slight reduction	Brantley et al. (2014) Chen et al. (2016) Tong et al. (2015) Viippola et al. (2018) Morakinyo et al. (2016)
	Combination of Tree and hedge	Mixed -20 to 40% Increase behind	Chen et al.(2016) Morakinyo et al. (2016)
Rapid: UFP	Hedge	High reduction: 37- 77%	Al-Dabbous and Kumar (2014)
	Tree	Mixed Reduction of 37.7-63.6%	Hagler et al. (2012) Lin et al. (2016)
Rapid: BC	Tree	Reduction of 7.8-12.4%	Brantley et al. (2014)
Rapid: CO	Tree	Reduction of 23.6-56.1%	Lin et al.(2016)
Rapid: NO_2	Tree	Reduction 14-59% Reduction 1-21% Average Reduction 7% Increase Increase	Fantozzi et al. (2015) Yin et al. (2011) Grundström and Pleijel (2014) Yli-Pelkonen et al. (2017) Viippola et al. (2018)
	Combination of Tree and hedge	Reduction	Klingberg et al. (2017)
O_3	Tree	Increase Non-significant reduction of 2%	Fantozzi et al. (2015) Grundström and Pleijel (2014)

Table 2. Details of six monitoring locations. Note the clear area and behind (CB) and in-front and behind (IB) monitoring points refer to measurements taken at a clear location adjacent to and in front of GI, respectively. In all cases, 'behind' refers to measurements carried out behind the GI, as explained in Figure 1. Leaf area index (LAI) is estimated with help of ceptometer Accu-PAR LP80. The superscript in column 1 describes the additional physical characteristics of the GI at each site. The superscript in column 5 describes the type and origin of the GI at each site.

GI Type (location)	Measurement locations (site abbreviation)	Road name (coordinates)	Approximate dimensions; L: Length, W:Width, H: Height	Species common name (*scientific name*)	LAI (hourly traffic)
Hedge only[1] (Aldershot road)	Clear and Behind (H_{CB})	A323 (51.251114, -0.599585)	L: 36m , W: 1m, H: 1.2m	Hawthorn (*Crataegus monogyna*)[a,c] Common Ivy (*Hedera helix*)[a,d]	LAI = 6.64 m^2/m^2 (750)
Hedge only[2] (Stoke park road)	In-front and Behind (H_{IB})	A320 (51.243999 -0.571478)	L: 36m, W: 1.5m, H: 2.2m	Beech (*Fagus sylvatica*)[a,c]	LAI = 4.47 m^2/m^2 (1200)
Tree only[3] (Aldershot road)	Clear and Behind (T_{CB})	A323 (51.250527, -0.597351)	L: 40m, W: 6m, H: 10m	Common lime (*Tilia x europaea*)[a,c]	LAI = 4.25m^2/m^2 (750)
Tree only[4] (Sutherland park)	In-front and Behind (T_{IB})	A3100 (51.261390, -0.547263	L: 50m, W: 9m, H: 7m	Common lime (*Tilia x europaea*)[a,c] Field maple (*Acer campestre*)[a,c] Poplar (*Populus nigra*) [a,c] Bird cherry (*Prunus padus*)[a,c]	LAI = 4.63 m^2/m^2 (1650)
Tree with hedge[5] (Sutherland park)	In-front and Behind (TH_{IB})	A3100 (51.260847, -0.546053**)**	L: ~40m, W: ~7m, H: ~5m	Hawthorn (*Crataegus monogyna*)[a,c] Common Ivy (*Hedera helix*)[a,d] Common Ash (*Fraxinus excelsior*) [a,c]	LAI = 1.54 m^2/m^2, LAI = 3.4 m^2/m^2 (1650)
Tree with hedge[6] (Shalford road)	Clear and Behind (TH_{CB})	A281 (51.227721, -0.571825)	L: ~66m W:~3.5m, H: ~4m	Red Pine (*Pinus resinosa*)[d] London plane (*Platanus x hispanica*)[b,c] blackthorn (*Prunus spinose*)[a,c]	LAI = 4.07 m^2/m^2 (1200)

[1]Hedge height is lower than breathing height; [2]Height is higher than average breathing levels; [3]Single tree row; the vertical distance between the bottom of tree crown and the ground surface ranged from 1.7-2.5m; [4] Multiple rows (up to 4) of tree in zig-zag planting formation; the vertical distance between the bottom of tree crown and the ground surface ranged from 1.0-2.5m; [5]Well maintained hedge of 1.7m height and single tree row behind the hedge; the vertical distance between the bottom of tree crown and the ground surface ranged from 1.5-2.5m; [6]Less maintained/ freely growing hedge with varying height 2-4 m; the trees are embedded in the hedgerows. [a]native; [b]non-native; [c]deciduous; [d]evergreen.

Table 3. The summary statistics showing the available number of one-minute averaged data points (N), median, geometric mean (GM) and geometric standard deviation (GSD) of pollutant concentration behind and in-front/clear measurement points at six monitoring sites and the relative difference in pollutant concentration. All these percentage calculations did not account for background subtraction and may underestimate our reported changes. The negative and positive values in the last column denotes decrease and increase in concentration behind GI, respectively.

		Clear area or In front of GI				**Behind GI**				**% diff**
		N	**median**	**GM**	**GSD**	**N**	**median**	**GM**	**GSD**	
BC	$\mathbf{H_{CB}}$	2159	654	541	2.7	2197	659	619	2.2	-15
	$\mathbf{T_{CB}}$	1587	743	531	4.2	1845	632	552	3.2	-4
	$\mathbf{TH_{CB}}$	2455	906	780	2.6	2550	913	747	2.5	4
	$\mathbf{H_{IB}}$	1931	1359	1218	2.9	1950	829	695	2.7	43
	$\mathbf{T_{IB}}$	2014	1213	1070	2.5	1977	852	594	3.7	44
	$\mathbf{TH_{IB}}$	1530	444	424	3.7	1557	173	155	6.0	63
PNC	$\mathbf{H_{CB}}$	2038	6322	6450	1.6	2024	5956	5877	1.6	9
	$\mathbf{T_{CB}}$	1799	5491	6149	1.6	1890	5797	6332	1.6	-3
	$\mathbf{TH_{CB}}$	1609	7678	7724	1.5	1562	8068	7854	1.5	-2
	$\mathbf{H_{IB}}$	1786	8190	8384	1.7	1786	5473	5880	1.6	30
	$\mathbf{T_{IB}}$	1919	11573	11081	1.6	1995	10983	10224	1.6	8
	$\mathbf{TH_{IB}}$	1161	4270	4629	1.6	1162	3722	3975	1.6	14
$\mathbf{PM_{10}}$	$\mathbf{H_{CB}}$	2375	17	15	1.6	2377	20	19	1.8	-22
	$\mathbf{T_{CB}}$	2009	16	16	1.6	1801	17	16	1.6	-2
	$\mathbf{TH_{CB}}$	2423	23	20	1.4	2424	20	19	1.5	7
	$\mathbf{H_{IB}}$	1948	16	16	1.4	1942	14	14	1.5	15
	$\mathbf{T_{IB}}$	2527	32	28	1.8	2527	27	25	1.8	10
	$\mathbf{TH_{IB}}$	1556	19	20	1.4	1557	15	15	1.7	24
$\mathbf{PM_{2.5}}$	$\mathbf{H_{CB}}$	2375	11	10	1.4	2377	11	11	1.4	-7
	$\mathbf{T_{CB}}$	2009	11	11	1.5	1801	12	12	1.4	-7
	$\mathbf{TH_{CB}}$	2423	16	15	1.4	2424	14	14	1.4	8
	$\mathbf{H_{IB}}$	1948	12	11	1.4	1942	10	10	1.4	14
	$\mathbf{T_{IB}}$	2527	24	20	1.9	2527	21	18	1.9	9
	$\mathbf{TH_{IB}}$	1556	13	14	1.4	1557	13	13	1.5	8
$\mathbf{PM_{1}}$	$\mathbf{H_{CB}}$	2375	6	6	1.3	2377	6	6	1.3	-1
	$\mathbf{T_{CB}}$	2009	7	7	1.4	1801	7	7	1.4	1
	$\mathbf{TH_{CB}}$	2423	12	12	1.4	2424	9	10	1.5	19
	$\mathbf{H_{IB}}$	1948	8	8	1.3	1942	6	6	1.5	25
	$\mathbf{T_{IB}}$	2527	14	12	1.7	2527	14	11	1.9	8
	$\mathbf{TH_{IB}}$	1556	8	8	1.4	1557	7	7	1.5	7